Clays and Clay Minerals, Vol. 52, No. 1, 85–105, 2004.

THE KÜBLER INDEX IN LATE DIAGENETIC TO LOW-GRADE METAMORPHIC PELITES: A CRITICAL COMPARISON OF DATA FROM 10 Å AND 5 Å PEAKS

STEFANO BATTAGLIA[1], LEONARDO LEONI[1,2,*] AND FRANCO SARTORI[2]

[1] Istituto di Geoscienze e Georisorse, (Consiglio Nazionale delle Ricerche), Area S. Cataldo, Via Moruzzi n.1, Pisa 56124, Italy
[2] Dipartimento di Scienze della Terra, Università di Pisa, Via S. Maria n. 53, Pisa 56126, Italy

Abstract—A set of 99 samples covering the whole range of low- and very low-grade metamorphic conditions has been used to compare Kübler index (KI) values measured on the illite 10 Å reflection ($KI_{10\,Å}$) with those obtained from the 5 Å reflection ($KI_{5\,Å}$). Evaluation of peak widths have been carried out both graphically on the recorded peak profiles from chart-strip X-ray diffraction (XRD) patterns and with the WINFIT computer program (Krumm, 1996) on fitted and decomposed profiles. All the measurements were performed both on air-dried and glycolated preparations. The data collected show that in the rock samples where illite is associated with significant amounts of I-S interstratified minerals, and/or K/Na intermediate micas, paragonite and other interfering phases, full width at half-maximum (FWHM) measurements on the 5 Å peak in fitted and decomposed XRD profiles from glycolated mounts give more reliable KI values than those obtained from the 10 Å peak. This is because of the easier and more complete de-summation of the illite second reflection from the contributions of all the interfering phases. In each sample population in which the rocks have the same metamorphic grade, $KI_{5\,Å}$ values from fitted and decomposed profiles show much lower scattering in comparison with $KI_{10\,Å}$ values and appear consistent with the values measured in lithologies without interfering phases.

The relationship between $KI_{10\,Å}$ and $KI_{5\,Å}$ appears very close to a 1:1 linear relationship; nevertheless, the conversion from $KI_{5\,Å}$ to $KI_{10\,Å}$ through the appropriate equation ($KI_{10\,Å} = KI_{5\,Å} \times 0.965 + 0.023°2\theta$) is recommended in order to avoid a small, but systematic, error.

In the range from late diagenesis to middle anchizone, where several phases may give diffraction effects interfering with illite peaks, the proposed procedure (*i.e.* FWHM measurements on the 5 Å peak in fitted and decomposed XRD profiles from glycolated mounts) seems to allow better estimates of the metamorphic grade than those obtained through traditional KI measurements.

Key Words—10 Å and 5 Å Peaks, Air-dried and EG-solvated Preparations, Fitted or Fitted and Decomposed Peaks, Illite, Kübler Index, Late Diagenesis, Low-grade Metamorphism, Metapelites.

INTRODUCTION

Since the studies of Weaver (1960) and Kübler (1964) the illite 'crystallinity' method has been used widely to determine diagenetic and very low-grade metamorphic zones in pelitic and marly rocks (Frey and Robinson, 1999, and references therein). As proposed by Kübler (1964, 1967, 1984), this method involves measuring the full width at half-maximum (FWHM) height of the illite 10 Å XRD peak in $°\Delta 2\theta$ CuKα units on patterns of air-dried (AD) samples. Over the following two decades, this parameter, called the Kübler index (KI) (Guggenheim *et al.*, 2002), was applied without significant modifications or improvements. During the past ten years, several attempts have been made to the interlaboratory correlation of KI measurements by selecting the optimal XRD instrumental conditions (Kisch, 1990), by defining standard sample preparation techniques (Kisch and Frey, 1987; Kisch, 1991; Krumm and Buggisch, 1991; Krumm, 1992), by verifying the precision and reproducibility of the KI measurements (Robinson *et al.*, 1990), and by providing interlaboratory standards with procedures for sample preparation and measurement conditions (Krumm *et al.*, 1994; Warr and Rice, 1994).

In this period there has also been a new awareness of the effects of disruptive factors connected with XRD interfering phases associated with illite. Frey (1987) had already warned about the presence of such minerals as paragonite and margarite and concluded that rock samples that contain these phyllosilicates (either as discrete phases or interstratifications) should be excluded. Subsequently, it has been widely recognized that in routine, serial XRD studies, reliable KI determinations may be severely hindered also by the association of illite with smectitic mixed-layer minerals (such as I-S or Chl-S) and/or with intermediate K/Na-rich micas (Árkai, 2002). These associations are much more frequent than those of illite with paragonite or margarite, particularly at diagenetic and low anchizonal grades. They produce XRD patterns showing a considerable broadening and shift of illite peaks, even when the interfering phases are present in small amounts. To eliminate these effects, various methods have been applied. The effects of smectitic interstratifications have frequently been eliminated by glycolation and/or decomposition of the basal reflections, while those

* E-mail address of corresponding author:
leoni@dst.unipi.it
DOI: 10.1346/CCMN.2004.0520109

Copyright © 2004, The Clay Minerals Society

https://doi.org/10.1346/CCMN.2004.0520109 Published online by Cambridge University Press

connected with intermediate K/Na-rich micas were necessarily removed only through decomposition techniques (Árkai, 2002, and references therein). Traditionally, KI measurements have been performed on the illite first basal reflection around 10 Å, both because of its higher intensity and because Kübler's original KI scale (on which the petrogenetic applications are still based) was established on FWHM values measured on it. However, this peak is the one most affected by partial to nearly complete overlap by other phases, such as smectitic interstratified phases and intermediate K/Na-rich micas. This was recognized by several authors (*e.g.* Lanson and Champion (1991), Stern *et al.* (1991), Lanson and Besson (1992), Velde and Lanson (1993), Wang *et al.* (1995)), who proposed various methods to decompose the so-called 'near-10 Å band' or 'complex peak in the range of 14 Å–10 Å'. Illite higher-angle basal peaks have rarely been taken into consideration for KI measurements (Nieto and Sanchez-Navas, 1994; Warr, 1996), probably because of the low intensities of these reflections and because they also are not completely free of overlap by other phases (*e.g.* 5 Å peak with chlorites, 3.3 Å peak with quartz, *etc.*). It is, however, undeniable that in these higher-order reflections the overlapping effects are less numerous, mostly partial, and easier to unravel.

In the present paper, we compare the KI values measured on the illite first reflection ($KI_{10\,Å}$) with those obtained from the second peak ($KI_{5\,Å}$), after application of decomposition techniques, in a set of rock samples covering the whole range of low- to very low-grade metamorphic conditions. These samples display considerable variation in the identity and amounts of minor phyllosilicate phases associated with dominant illite and chlorite and constitute excellent material for testing the ability of decomposition techniques, coupled with sample glycolation, to unravel complex multi-phase peaks. The main purpose of the work is to prove that the second basal reflection of illite may allow more reliable measurements of KI than those obtained from the first reflection, especially in the late diagenesis-low anchizone realm, where smectitic interstratified phases and intermediate K/Na-rich micas may be particularly abundant.

EXPERIMENTAL

Samples

The 99 samples studied in the present work were chosen from several hundreds investigated for metamorphic petrogenetic studies in the Department of Earth Sciences at Pisa University (Italy). They were selected to cover a wide range of 'crystallinity' from diagenesis to early epizone and to present a marked variation in clay mineral assemblages.

These samples were collected from ten different tectonic units: eight of them belong to the Northern Apennines chain (Italy), one unit belongs to the metamorphic basement of southern Sardinia (Italy), and the other represents a part of the Carpathian belt in Romania. In most units only one formation has been sampled, whereas in the Tuscan Nappe Unit three different formations have been considered. Some formations, such as Palombini Shale and Tuscan Scaglia, are present in various units.

All the samples from the same unit are supposed to have the same metamorphic grade (as the difference between their structural depths is always relatively small) and to form a single sample population. Detailed information on such populations is given in the Appendix to the present work, which can be viewed at the Internet site: http://www.dst.unipi.it/min/clay; the main features (including the clay mineral assemblage of each sample) are reported in Table 1.

Methods

Rock samples were disaggregated under standard conditions using a jaw crusher and then gently crushed in a mortar mill for ~3 min. Previous studies showed that this short-term pulverization had no measurable effects on the KI values (Árkai *et al.*, 1995). Bulk-rock mineral assemblages were determined from XRD patterns of unoriented whole-rock powders. Clay mineral assemblages and KI indices were determined from XRD patterns of highly oriented <2 μm grain-size fractions. Such fractions were separated from the aqueous suspensions of the whole-rock powders by differential settling. The aqueous suspension of the given fraction was pipetted, saturated with Sr^{2+} and dried at room temperature on a glass slide to produce highly oriented preparations. Care was taken to avoid thin preparations; the amount of clay on each slide was in the range of 3–4 mg/cm^2 (Lezzerini *et al.*, 1995). No preliminary treatment was applied to remove carbonates, which are common in many of the studied samples, or organic matter present in moderate amounts in some samples. These treatments were avoided as they may have deleterious effects on the small-sized phyllosilicates.

The XRD patterns were recorded using a Philips PW1710 automatic diffractometer, equipped with a long fine-focus Cu tube, at the following instrumental settings: CuKα Ni-filtered radiation; 40 kV; 20 mA; slits: ½° divergence and scatter, 0.2 mm receiving; continuous scanning; scan speed: 0.25°2θ per minute; time constant: 4 s. Each XRD slide preparation was scanned both in the air-dried (AD) and glycolated (EG) states from 3 to 21°2θ. To identify the nature of illite-smectite mixed-layer minerals (ratio of component layers and type of interstratification) for a selected number of samples, AD and EG Na-saturated preparations were run from 3 to 40°2θ (Środoń, 1984).

Evaluation of FWHM values was done both off-line graphically on chart-strip XRD patterns and with a computer on background-subtracted reflections. Various

https://doi.org/10.1346/CCMN.2004.0520109 Published online by Cambridge University Press

https://doi.org/10.1346/CCMN.2004.0520109 Published online by Cambridge University Press

Table 1. $KI_{10\ Å}$ and $KI_{5\ Å}$ values of the studied samples, their sources, metamorphic grades, bulk-rock and clay mineral assemblages (Sm. No = sample number; AD = values from air-dried preparations; EG = values from ethylene glycol-solvated preparations. Bold type = values determined graphically on chart-strip diffraction patterns. Italic type = values evaluated on fitted or on 'fitted and decomposed' profiles by using WINFIT program (Krumm, 1996)).

Rock source	Metam. zone†	Bulk-rock mineral assemblage	Sm. No	$KI_{10\ Å}$ (°2θ) AD	$KI_{10\ Å}$ (°2θ) EG	$KI_{5\ Å}$ (°2θ) AD	$KI_{5\ Å}$ (°2θ) EG	Clay mineral assemblage
Population 1:								
Riu Gruppa/Castello	Epizone	Qtz + Fs + I ± Chl ± Pg	1	*0.13*	*0.14*	*0.12*	*0.12*	I + Chl
Medusa Unit		± Cld	2	*0.15*	*0.16*	*0.13*	*0.13*	I + Chl
(Metamorphic basement of Sardinia,			3	*0.15*	*0.14*	*0.12*	*0.13*	I + Chl
Sardinian Variscides, SE Sardinia, Italy)			4	*0.15*	*0.14*	*0.14*	*0.13*	I + Chl
Mandas Complex Formation			5	*0.15*	*0.14*	*0.14*	*0.14*	I + Chl
			6	*0.17*	*0.17*	*0.17*	*0.16*	I + Chl
			7	*0.18*	*0.18*	*0.18*	*0.17*	I + Chl
			8	*0.19*	*0.19*	*0.16*	*0.16*	I + Chl + Pg*
			9	*0.20*	*0.21*	*0.17*	*0.17*	I
			10	*0.21*	*0.22*	*0.19*	*0.20*	I + Chl
			11	*0.21*	*0.21*	*0.20*	*0.19*	I + Chl
			12	*0.22*	*0.21*	*0.19*	*0.18*	I + Chl
			13	*0.26*	*0.25*	*0.23*	*0.24*	I + Chl
Population 2:								
S. Maria del Giudice Unit	Epizone	Qtz + Cal ± Fs + I ± Chl	14	*0.18*	*0.17*	*0.15*	*0.15*	I + Chl
(Tuscan Domain Units, Monti Pisani,			15	*0.19*	*0.19*	*0.16*	*0.16*	I + Chl
N Apennines, NW Tuscany, Italy)			16	*0.20*	*0.21*	*0.20*	*0.20*	I + Chl
Tuscan Scaglia Formation			17	*0.20*	*0.21*	*0.19*	*0.18*	I + Chl
			18	*0.22*	*0.22*	*0.20*	*0.20*	I + Chl
			19	*0.22*	*0.22*	*0.22*	*0.20*	I
			20	*0.22*	*0.24*	*0.21*	*0.22*	I + Chl
			21	*0.22*	*0.21*	*0.21*	*0.21*	I
			22	*0.27*	*0.26*	*0.24*	*0.25*	I + Chl
			23	*0.27*	*0.25*	*0.24*	*0.23*	I + Chl
Population 3:								
Monte Serra Unit	Epizone	Qtz + Fs + I ± Chl ± Prl	24	*0.19*	*0.18*	*0.17*	*0.17*	I
(Tuscan Domain Units, Monti Pisani,		± Pg	25	*0.20*	*0.19*	*0.19*	*0.20*	I + Chl + Pg*
N Apennines, NW Tuscany, Italy)			26	*0.21*	*0.21*	*0.18*	*0.20*	I + Chl + Pg*
Verruca Formation			27	*0.21*	*0.21*	*0.18*	*0.19*	I
(Scisti Violetti Member)			28	*0.22*	*0.20*	*0.19*	*0.19*	I + Chl
			29	*0.22*	*0.23*	*0.20*	*0.20*	I
			30	*0.22*	*0.21*	*0.21*	*0.20*	I
			31	*0.23*	*0.24*	*0.23*	*0.23*	I + Chl + Prl*
			32	*0.24*	*0.24*	*0.24*	*0.24*	I + Chl + Pg*
			33	*0.25*	*0.26*	*0.25*	*0.25*	I + Chl
			34	*0.26*	*0.25*	*0.24*	*0.24*	I + Chl +Pg*
			35	*0.26*	*0.26*	*0.24*	*0.25*	I + Chl

https://doi.org/10.1346/CCMN.2004.0520109 Published online by Cambridge University Press

Table 1. (*contd.*)

Rock source	Metam. zone†	Bulk-rock mineral assemblage	Sm. No	$KI_{10\ Å}$ (°2θ) AD	$KI_{10\ Å}$ (°2θ) EG	$KI_{5\ Å}$ (°2θ) AD	$KI_{5\ Å}$ (°2θ) EG	Clay mineral assemblage
Population 4:								
Cravasco/Voltaggio Unit (Internal Ligurid Units, N Apennines, central Liguria, Italy)	Epizone	Qtz + Cal + Pl + l + Chl + Pg	36	*0.19*	*0.18*	*0.18*	*0.18*	I + Chl + Pg*
			37	*0.19*	*0.19*	*0.18*	*0.18*	I + Chl + Pg*
			38	*0.23*	*0.22*	*0.22*	*0.22*	I + Chl + Pg*
Palombini Shale Formation			39	*0.25*	*0.25*	*0.24*	*0.24*	I + Chl + Pg*
Population 5:								
Monte Figogna Unit (Internal Ligurid Units, N Apennines, central Liguria, Italy)	Anchizone/ epizone transition	Qtz + Cal + Pl + I + Chl + Pg	40	**0.30**–*0.26*	**0.31**–*0.25*	*0.26*	*0.27*	I + Chl + Pg**
			41	**0.30**–*0.27*	**0.31**–*0.27*	*0.26*	*0.28*	I + Chl + Pg** + K/Na mica (?)
			42	**0.33**–*0.29*	**0.34**–*0.28*	*0.28*	*0.29*	I + Chl + Pg**
Palombini Shale Formation			43	**0.35**–*0.30*	**0.34**–*0.30*	*0.29*	*0.30*	I + Chl + Pg**
Population 6: **Tuscan Nappe Unit** (Tuscan Domain Units, La Spezia megafold, N Apennines, SE Liguria, Italy)								
Posidonomya Marl Formation	Anchizone	Qtz + Cal + Fs + I + Chl	44	*0.24*	*0.24*	*0.23*	*0.22*	I + Chl
			45	*0.25*	*0.24*	*0.22*	*0.22*	I + Chl
			46	*0.25*	*0.26*	*0.23*	*0.22*	I + Chl
			47	*0.25*	*0.26*	*0.24*	*0.25*	I + Chl
			48	*0.26*	*0.25*	*0.24*	*0.23*	I + Chl
			49	*0.26*	*0.27*	*0.23*	*0.24*	I + Chl
			50	*0.27*	*0.26*	*0.24*	*0.23*	I + Chl
			51	*0.28*	*0.28*	*0.25*	*0.24*	I + Chl
Rhaetavicula contorta Limest. and Marl Formation	Anchizone	Qtz + Cal + Fs + I ± Chl ± I-S ± K/Na mica	52	*0.27*	*0.27*	*0.25*	*0.26*	I + Chl
			53	*0.29*	*0.28*	*0.28*	*0.27*	I + Chl
			54	**0.29**–*0.27*	**0.27**–*0.25*	*0.25*	*0.26*	I + Chl + K/Na mica?
			55	*0.31*	*0.30*	*0.27*	*0.27*	I + Chl
			56	**0.34**–*0.32*	**0.32**–*0.30*	*0.27*	*0.28*	I + Chl + K/Na mica*
			57	**0.38**–*0.33*	**0.36**–*0.31*	*0.29*	*0.30*	I + K/Na mica**
			58	**0.32**–*0.26*	**0.33**–*0.26*	*0.28*	*0.28*	I + Chl + K/Na mica**
			59	**0.42**–*0.31*	**0.41**–*0.29*	*0.37*	**0.40**–*0.29*	I + Chl + l-S*
			60	**0.40**–*0.30*	**0.39**–*0.28*	*0.38*	**0.41**–*0.28*	I + Chl + l-S*
Tuscan Scaglia Formation	Anchizone	Qtz + Cal + Fs + I + Chl ± I-S	61	**0.36**–*0.28*	**0.35**–*0.27*	**0.32**–*0.27*	**0.33**–*0.26*	I + Chl + K/Na mica*+ l-S?
			62	**0.44**–*0.26*	**0.42**–*0.26*	**0.34**–*0.27*	**0.37**–*0.27*	I + Chl + K/Na mica*+ l-S?
			63	**0.44**–*0.26*	**0.40**–*0.28*	**0.35**–*0.27*	**0.38**–*0.28*	I + Chl+ K/Na mica* + I-S?
			64	**0.45**–*0.26*	**0.42**–*0.28*	**0.28**–*0.26*	**0.31**–*0.27*	I + Chl+ K/Na mica* + l-S?
			65	**0.50** -*0.29*	**0.40**–*0.27*	**0.32**–*0.28*	**0.36**–*0.27*	I +Chl+ K/Na mica* + I-S*
			66	**0.62**–*0.30*	**0.58**–*0.27*	**0.37**–*0.28*	**0.39**–*0.29*	I + Chl+ K/Na mica **+ l-S*
			67	**0.59**–*0.29*	**0.50**–*0.30*	**0.40**–*0.29*	**0.46**–*0.30*	I + Chl+K/Na mica **+ I-S*
			68	**0.75**–*0.30*	**0.56**–*0.29*	**0.38**–*0.32*	**0.52**–*0.30*	I + Chl + K/Na mica **+ l-S**

https://doi.org/10.1346/CCMN.2004.0520109 Published online by Cambridge University Press

Population 7:								
Monte Gottero Unit	Anchizone	Qtz + Cal + Pl + I + Chl	69	*0.34*	*0.35*	*0.31*	*0.33*	I + Chl + K/Na mica?
(Internal Ligurid Units, N Apennines		± I-S ± Pg? ± K/Na mica?	70	*0.36*	*0.34*	*0.34*	*0.35*	I + Chl
E Liguria, Italy)			71	**0.35**–*0.37*	*0.34*	*0.33*	*0.34*	I + Chl + I-S?
Palombini Shale Formation			72	*0.40*	*0.38*	*0.36*	*0.38*	I + Chl
			73	*0.41*	*0.39*	**0.38**–*0.36*	**0.40**–*0.37*	I + Chl+ Pg?
			74	**0.51**–*0.35*	**0.44**–*0.32*	*0.33*	**0.43**–*0.33*	I + Chl + I-S*
			75	**0.51**–*0.36*	**0.45**–*0.33*	*0.34*	**0.44**–*0.32*	I + Chl+ I-S*
Population 8:								
Fenes Nappe Unit	Diagenesis	Qtz + Cal + Fs + l ± I-S?	76	*0.42*	*0.40*	*0.38*	*0.41*	I + Chl
(Cretaceous Flysch Units, S Apuseni			77	**0.44**–*0.46*	**0.40**–*0.42*	**0.42**	**0.42**–*0.44*	I + Chl + I-S?
Mts, Carpathians, Romania)			78	*0.47*	*0.46*	*0.43*	*0.45*	I + Chl
Fenes Formation			79	**0.50**–*0.52*	*0.49*	**0.50**	**0.50**–*0.52*	I + Chl + I-S?
			80	*0.52*	*0.50*	*0.47*	*0.52*	I + Chl
			81	**0.52**–*0.54*	**0.50**–*0.52*	*0.47*	*0.49*	I + Chl + I-S?
Population 9:								
Bracco/Val Graveglia Unit	Diagenesis	Qtz + Cal + Pl + I + Chl	82	*0.46*	*0.45*	*0.39*	*0.45*	I + Chl
(Internal Ligurid Units, N Apennines		± I-S ± K/Na mica	83	*0.45*	*0.44*	*0.40*	*0.44*	I + Chl
E Liguria, Italy)			84	**0.58**–*0.42*	**0.50**–*0.40*	0.43	**0.51**–*0.41*	I + Chl + I-S*
Palombini Shale Formation			85	**0.60** -*0.44*	**0.53**–*0.39*	0.47	**0.55**–*0.43*	I + Chl + I-S*
			86	**0.60**–*0.45*	**0.55**–*0.45*	0.44	**0.56**–*0.45*	I + Chl + I-S*
			87	**0.64**–*0.48*	**0.58**–*0.48*	**0.53**–0.47	**0.64**–*0.46*	I + Chl + K/Na mica *+ I-S*
			88	**0.65**–*0.41*	**0.54**–*0.40*	0.41	**0.56**–*0.39*	I + Chl +K/Na mica? + I-S**
			89	**0.66**–*0.42*	**0.56**–*0.40*	0.45	**0.58**–*0.42*	I + Chl + I-S**
			90	**0.80**–*0.45*	**0.65**–*0.46*	0.50	**0.64**–*0.46*	I + Chl + I-S***
Population 10:								
Upper Ophiolitiferous Unit	Diagenesis	Qtz + Cal + Pl + I + I-S	91	**0.47**–*0.38*	**0.40**–*0.37*	0.39	**0.50**–*0.36*	I + Chl+ l-S*
(Internal Ligurid Units, Monti di		± Chl-S ?	92	**0.64**–*0.36*	**0.50**–*0.36*	0.43	**0.49**–*0.37*	I + Chl+ l-S*
Castellina Marittima, N Apennines			93	**0.85**–*0.40*	**0.54**–*0.40*	0.49	**0.63**–*0.39*	I + Chl+ l-S**
SW Tuscany, Italy)			94	**0.90**–*0.39*	**0.50**–*0.38*	0.46	**0.64**–*0.36*	I + Chl+ l-S**
Palombini Shale Formation			95	**1.02**–*0.42*	**0.50**–*0.38*	0.48	**0.65**–*0.37*	I + Chl+ l-S**
			96	**1.02**–*0.38*	**0.58**–*0.38*	0.47	**0.66**–*0.36*	I + Chl+ l-S**+ Chl-S?
			97	**n.m.**–**0.41**	**0.60**–*0.38*	0.50	**0.80**–*0.40*	I + Chl+ l-S***+ Chl-S?
			98	**n.m.**–*0.42*	**0.60**–*0.40*	0.45	**n.m.**–*0.39*	I + Chl+ l-S***
			99	**n.m.**–*0.40*	**0.51**–*0.37*	0.47	**n.m.**–*0.38*	I + Chl+ l-S***

† Metamorphic zone derived from literature (see Appendix at Internet site: http://www.dst.unipi.it/min/clay)

All mineral abbreviations except for feldspars (Fs), illite (I), illite-smectite (I-S), chlorite-smectite (Chl-S) and intermediate K/Na mica (K/Na mica) after Kretz (1983)

* scarce to moderately abundant; ** abundant; *** very abundant; ? questionable; n.m. = not measurable

mathematical functions are, in principle, able to fit a diffraction curve. However, Stern *et al.* (1991) found that Pearson functions are particularly recommended when peaks of various heights have to be fitted. Therefore, the computer-based evaluation was done using Krumm's (1996) WINFIT program which determines the peak's FWHM by first subtracting the background from the raw data, then operating the peak fitting through a Pearson VII function. Peaks at low angles (within the range 5–10°2θ CuKα; 17.6–8.8 Å) were fitted simultaneously or as single peaks (depending on the clay mineral assemblage) through an asymmetric function. In contrast, peaks at higher angles (within the range 16.50–19.50°2θ CuKα; 5.3–4.5 Å) were fitted simultaneously through a symmetrical Pearson VII function in order to reduce the number of parameters to be refined. This approximation seems acceptable, since at these angles the shape of a single-phase peak appears, at most, only slightly asymmetrical. Only for sample 98, which contains the greatest amount of I-S mixed-layer minerals having the highest percentage of smectitic layers, was application of an asymmetric function required.

The number of elementary curves applied in the decomposition process was fixed on the basis of very careful assumptions. For AD profiles, the procedure has been to increase the number of curves progressively in order to get a good fit with the smallest possible number of elementary peaks; this was found to be no greater than the number of clay mineral phases recognized in the qualitative analysis of the whole XRD profile (both AD and EG) from 3 to 50°2θ. Therefore, decomposition of AD profiles involved association of a single curve to each mineral phase (except in the cases where a perfect overlap occurs, as for illite and I-S contributions in the 5 Å peak region (for more detail, see the paragraph concerning the I-S phase-bearing assemblages)). For EG profiles, the number of elementary peaks is a function of both the number of phases found for the AD profile, and of the assumed nature of the associated phases (expandable or not). For example, when expandable I-S phases are present, the EG 10 Å peak decomposition requires a new peak in addition to those found in the AD profiles, because a doublet is associated with glycolated I-S mixed-layer phases in this angular range (one peak on each side of 10 Å) (Lanson and Besson, 1992).

Various peak-fitting trials, in which the $K\alpha_2$ wavelength was retained, were performed; this produced suitable fitted profiles, on which $KI_{10\,Å}$ and $KI_{5\,Å}$ parameters were measured.

For a large number of samples, statistical parameters of the measurements were evaluated from runs of several slides prepared from the same suspension of a given sample. This test showed that the relative standard deviation of the FWHM measurements is in the range 3–5% for the samples having the (illite ± chlorite) clay mineral assemblage, whereas it is in the range 5–8% for the samples containing I-S interstratified minerals and/or K/Na intermediate micas. As expected, the largest values were observed in the samples having the largest amounts of these interfering phases.

The KI values presented in this paper are not calibrated either to Kübler's scale (Kübler, 1967) or to the CIS scale (Warr and Rice, 1994). The conversions can be done easily by applying the following equations: $KI_{Kübler} = KI_{Pisa} \times 1.08 + 0.01°2\theta$; $KI_{CIS} = KI_{Pisa} \times 1.09 + 0.05°2\theta$ (Leoni, 2001).

RESULTS AND DISCUSSION

The data collected in the present study are reported in Tables 1, 2 and 3 and illustrated in Figures 1 to 7. Table 1 gives the $KI_{10\,Å}$ and $KI_{5\,Å}$ values (both determined in AD and EG conditions) for each sample. Samples are separated into ten populations as a function of their rock source; such groups are listed in order of decreasing metamorphic grade (epizone → anchizone → diagenesis), as given in the literature (see Appendix at the Internet site: http://www.dst.unipi.it/min/clay); within each metamorphic zone different sample populations and single samples are arranged in order of increasing $KI_{10\,Å}$ (AD) values. Both values measured graphically on chart-strip XRD patterns (bold type) and computer-based values measured on fitted or on 'fitted and decomposed' profiles (italic type) are reported; when the difference between the two values is <0.02°2θ, only the computer-based value is given. As the problems to be dealt with in the decomposition of complex peaks are basically the same for all the samples having a given clay mineral assemblage, presentation and discussion of data hereafter will be done as a function of such assemblages.

Measurement of $KI_{10Å}$ and $KI_{5Å}$ in (illite Ô chlorite) clay mineral assemblages

The XRD patterns of samples containing only illite obviously do not present any problem of interference for both the mica's first and second basal peaks. The samples having illite and chlorite as clay minerals show XRD patterns whose illite 001 peak is still free from interferences, whereas the mica 002 reflection appears partially overlapped by the chlorite 003 reflection (for illite and chlorite the indices of reflections will be referred to hereafter as the 10 Å polytype cell and the 14 Å polytype cell, respectively). These two latter reflections, however, differ in angular position by ~1°2θ (for CuKα radiation) allowing easy decomposition of their contributions through a simultaneous fitting procedure. Also, this wide difference in angular position makes it possible to perform graphical measurements on mica peaks which are not significantly affected by the partial overlap with chlorite reflections. This makes graphically-derived and computer-measured KI values identical (differences are <0.02°2θ); therefore, only the

https://doi.org/10.1346/CCMN.2004.0520109 Published online by Cambridge University Press

https://doi.org/10.1346/CCMN.2004.0520109 Published online by Cambridge University Press

Table 2. Środoń (1984) parameters for the identification of illitic materials in a selected number of samples (Sm. No = sample number; bold type = values determined graphically on chart-strip XRD patterns; italic type = values evaluated on fitted or on fitted and decomposed profiles by using WINFIT program (Krumm, 1996)).

Sm. No	Metam. zone[†]	Reflections from glycolated mounts (°2θ, CuKα radiation)								$\Delta_{002-001}$ (°2θ)		BB1[1] (°2θ")	BB2[1] (°2θ)	Ir[1]	%S[2] in I-S		Type of illitic material
		I-S	I 001[3]	I-S	I 002	I-S	I + I-S 003	I-S	I 004	I	I-S				A	B	
(illite + chlorite) clay mineral assemblage																	
52	Anchiz.	abs.	*8.85*	abs.	*17.74*	abs.	*26.78*	abs.	*35.96*	*8.89*	–	**2.3**	**1.3**	**1.02**	–	–	I
76	Diagen.	abs.	*8.86*	abs.	*17.71*	abs.	*26.76*	abs.	*35.94*	*8.85*	–	**2.4**	**1.3**	**1.10**	–	–	I + ISII (tr?)
80	Diagen.	abs.	*8.84*	abs.	*17.72*	abs.	*26.75*	abs.	*35.95*	*8.88*	–	**2.5**	**1.3**	**1.10**	–	–	I + ISII (tr?)
(illite + chlorite + paragonite) clay mineral assemblage																	
36	Epiz.	abs.	*8.84*	abs.	*17.76*	abs.	*26.78*	abs.	*35.96*	*8.92*	–	**1.9**	**1.4**	**1.05**	–	–	I
42	Epiz/Anch.	abs.	*8.83*	abs.	*17.73*	abs.	*26.77*	abs.	*35.98*	*8.90*	–	**2.1**	**1.3**	**0.99**	–	–	I
(illite + chlorite + illite-smectite) clay mineral assemblage																	
74	Anchiz.	abs.	*8.86*	*8.93*	*17.74*	*17.60*	*26.78*	*35.05*	*35.96*	*8.88*	*8.67*	**2.8**	**2.2**	**1.15**	*5*	*6Ô3*	I + ISII
85	Diagen.	*8.15 b*	*8.84*	*8.99*	*17.71*	*17.61*	*26.78*	*34.95*	*35.94*	*8.87*	*8.62*	**2.8**	**2.6**	**1.31**	*5*	*9Ô3*	I + ISII
89	Diagen.	*8.20 b*	*8.86*	*8.97*	*17.72*	*17.59*	*26.77*	*34.85*	*35.98*	*8.86*	*8.62*	**3.1**	**3.0**	**1.45**	*5*	*10Ô3*	I + ISII
90	Diagen.	*8.05 b*	*8.86*	*9.05*	*17.70*	*17.58*	*26.78*	*34.96*	*35.93*	*8.84*	*8.53*	**3.0**	**3.0**	**1.29**	*5*	*9Ô3*	I + ISII
93	Diagen.	*7.60 b*	*8.85*	*9.10*	*17.71*	*17.25*	*26.75*	*34.85*	*35.95*	*8.86*	*8.15*	**3.4**	**2.9**	**1.25**	*16*	*10Ô3*	I + ISII
98	Diagen.	*7.60 b*	*8.85*	*9.07*	*17.73*	*17.20*	*26.76*	*34.70*	*35.96*	*8.88*	*8.13*	**3.7**	**3.0**	**1.40**	*17*	*12Ô3*	I + ISII
(illite + chlorite + K/Na mica + illite-smectite) clay mineral assemblage																	
66	Anchiz.	*7.60 b*	*8.84*	*9.12*	*17.73*	*17.42*	*26.75*	*35.07*	*35.95*	*8.89*	*8.30*	**3.0**	**2.8**	**1.20**	*11*	*6Ô3*	I + ISII
68	Anchiz.	*7.60 b*	*8.85*	*9.14*	*17.72*	*17.40*	*26.77*	*34.80*	*35.96*	*8.87*	*8.26*	**3.5**	**2.8**	**1.28**	*12*	*11Ô3*	I + ISII
87	Diagen.	*7.90 b*	*8.81*	*9.00*	*17.70*	*17.38*	*26.75*	*34.95*	*35.98*	*8.89*	*8.38*	**3.3**	**2.8**	**1.33**	*13*	*9Ô3*	I + ISII

[†] Metamorphic zone derived from literature (see Appendix at Internet site: http://www.dst.unipi.it/min/clay)

[1] These indices are explained in the text and in the paper by Środoń (1984)

[2] Percentage of smectite in the I-S mixed-layer mineral as established through plots based on Figure 2 (column A) or on Figure 7 (column B) of Środoń (1984)

[3] Indices of reflections are referred to 1-layer polytypes.

b = broad; abs. = absent; - = not measurable, since the phase is absent or questionable; tr? = questionable trace

I = illite; I-S = illite-smectite; S = smectite

Table 3. Average KI values of the studied sample sets (or sub-sets for population 6) (AD = values from air-dried preparations: EG = values from ethylene glycol-solvated preparations. Bold type = values determined graphically on chart-strip XRD patterns; italic type = values evaluated on fitted or on fitted and decomposed profiles by using WINFIT program (Krumm, 1996)).

Rock source	Metam. zone†	$KI_{10\ Å}$ (°2θ) AD	$KI_{10\ Å}$ EG	$KI_{5\ Å}$ (°2θ) AD	$KI_{5\ Å}$ EG	$KI_{10\ Å}$* (°2θ)	A $KI_{10\ Å}$** (°2θ)	B $KI_{10\ Å}$‡ (°2θ)	Metam. zone¶
Population 1: **Riu Gruppa/Castello Medusa Unit** ***Mandas Complex Form.***	Epizone	*0.18*	*0.18*	*0.16*	*0.16*	*0.18*	*0.20*	**0.20**	Epizone
Population 2: **S. Maria del Giudice Unit** ***Tuscan Scaglia Form.***	Epizone	*0.22*	*0.22*	*0.20*	*0.20*	*0.22*	*0.25*	**0.25**	Epiz./anchiz. transition
Population 3: **Monte Serra Unit** ***Verruca Form.*** ***(Scisti Violetti Member)***	Epizone	*0.23*	*0.22*	*0.21*	*0.21*	*0.23*	*0.26*	**0.26**	Epiz./anchiz. transition
Population 4: **Cravasco/Voltaggio Unit** ***Palombini Shale Form.***	Epizone	*0.22*	*0.21*	*0.21*	*0.21*	*0.23*	*0.26*	**0.25**	Epiz./anchiz. transition
Population 5: **Monte Figogna Unit** ***Palombini Shale Form.***	Epiz./anchiz. transition	**0.32** – *0.28*	**0.32** – *0.28*	*0.27*	*0.28*	*0.29*	*0.32*	**0.36**	Anchizone
Population 6: **Tuscan Nappe Unit** ***Posidonomya Marl Form.***	Anchizone	*0.26*	*0.26*	*0.24*	*0.23*	*0.24*	*0.27*	**0.29**	Anchizone
Rhaetavicula contorta Limest. and Marl Form.	Anchizone	**0.34** – *0.30*	**0.33** – *0.29*	*0.29*	**0.31** – *0.28*	*0.29*	*0.32*	**0.38**	Anchizone
Tuscan Scaglia Form.	Anchizone	**0.52** – *0.28*	**0.45** – *0.28*	**0.34** – *0.28*	**0.39** – *0.28*	*0.29*	*0.32*	**0.57**	Anchizone
Population 7: **Monte Gottero Unit** ***Palombini Shale Form.***	Anchizone	**0.41** – *0.37*	**0.38** – *0.35*	**0.34** – *0.34*	**0.38** – *0.35*	*0.36*	*0.40*	**0.45**	Anchizone
Population 8: **Fenes Nappe Unit** ***Fenes Form.***	Diagenesis	**0.48** – *0.49*	**0.46** – *0.47*	*0.45*	**0.46** – *0.47*	*0.48*	*0.53*	**0.53**	Diagenesis
Population 9: **Bracco/Val Graveglia Unit** ***Palombini Shale Form.***	Diagenesis	**0.60** – *0.44*	**0.53** – *0.43*	**0.45** – *0.44*	**0.55** – *0.43*	*0.44*	*0.49*	**0.66**	Diagenesis
Population 10: **Upper Ophiolitiferous Unit** ***Palombini Shale Form.***	Diagenesis	**0.82** – *0.39*	**0.53** – *0.38*	*0.46*	**0.62** – *0.38*	*0.39*	*0.43*	**0.90**	Anchiz./diag. transition

† metamorphic zone derived from literature (see Appendix at Internet site: http://www.dst.unipi.it/min/clay); same as in Tables 1 and 2
¶ metamorphic zone established on the basis of $KI_{10\ Å}$** data and the Kübler's scale limits (0.42 and 0.25 °2θ, for the lower and upper anchizone limit, respectively)
$KI_{10\ Å}$* = $KI_{10\ Å}$ value derived from $KI_{5\ Å\text{-}EG}$ value through application of the equation: $KI_{10\ Å} = KI_{5\ Å} \times 0.965 + 0.023°2\theta$ (see text)
$KI_{10\ Å}$** = $KI_{10\ Å}$ value derived from $KI_{10\ Å}$* value calibrated with respect to the Kübler's scale through application of the equation: $KI_{Kübler} = KI_{Pisa} \times 1.08 + 0.01$ °2θ
$KI_{10\ Å}$‡ = $KI_{10\ Å\text{-}AD}$ value determined graphically on chart-strip diffraction patterns and calibrated with respect to Kübler's scale through application of the equation:
$KI_{Kübler} = KI_{Pisa} \times 1.08 + 0.01°2\theta$

latter values have been reported in Table 1. Furthermore, differences between AD and EG values are commonly very small for both 001 and 002 peaks. For KI values in the range of 0.13–0.36°2θ (which correspond to epizonal and anchizonal samples) Kübler's scale (1967)), these differences are $\leqslant 0.02°2\theta$ (most commonly $\leqslant 0.01°2\theta$); they fall within precision limits (0.005–0.02°2θ) and are randomly distributed, as supported by the values of their algebraic sum calculated on all the 41 epizonal and anchizonal samples containing

https://doi.org/10.1346/CCMN.2004.0520109 Published online by Cambridge University Press

the illite ± chlorite assemblage, which are +0.10 and −0.01°2θ for the 10 Å and the 5 Å peaks, respectively.

For the samples having KI values >0.36°2θ (*i.e.* samples 72, 76, 78, 80, 82 and 83, which, according to Kübler's scale, belong to the diagenetic zone or to the transition between diagenesis and anchizone), the differences between indices measured in air-dried and ethylene glycol-solvated conditions are still very small for the 001 peak ($(KI_{AD\text{-}10\ Å} - KI_{EG\text{-}10\ Å}) \leqslant 0.02°2\theta$), but become significant for the 002 reflection ($(KI_{AD\text{-}5\ Å} - KI_{EG\text{-}5\ Å}) = 0.02–0.06°2\theta$). For these samples the contribution to the mica peaks of a discrete I-S mixed-layer phase or the presence of a few smectitic layers within the essentially illitic main phase may be suspected. Evidently, these swelling components are present in such small proportions that they could not be proved either by the fitting-decomposition procedure or by the parameters of Środoń's (1984) method; they are only revealed by a slight broadening of the mica 002 reflection following ethylene glycol solvation.

After the works of Lanson and Besson (1992) and Lanson (1997), many workers now decompose the diffraction maxima due to illitic material into two bands, one representing a sub-population of crystallites of low thickness and the other a sub-population of crystallites of high thickness.

Despite a full justification of this decomposition procedure by Lanson and Besson (1992), all throughout the present work it has been found more convenient to represent the purely illitic material with a unique curve on the grounds of the following considerations: (1) it is always desirable to fit the experimental data with as few elementary contributions as possible, because the fit always improves as more parameters are fitted; (2) the purpose of the present work is to achieve reliable KI measurements, which could be ascribed to a 'mean' illite population, relieved of effects due to interfering phases.

Measurement of $KI_{10Å}$ and $KI_{5Å}$ in (illite + chlorite + paragonite) and (illite Ô chlorite + intermediate K/Na mica) clay mineral assemblages

The presence of paragonite produces a broadening of the illite 001 peak which manifests itself as a high-angle tail (Figure 1a). When the Na-mica is not very abundant (as in all our samples) this tail is limited to the lower part of the illite peak so that it does not appreciably influence the graphical measurement of the FWHM peak. Should paragonite be very abundant, such graphical evaluation of $KI_{10\,Å}$ would become impossible and the peak-fitting decomposition procedure compulsory. Usually, a peak separation through the latter procedure is possible for whatever proportion of the two phases since the positions of their reflections differ by ~0.30°2θ and their FWHM by >0.2°2θ (Lanson, 1990; Lanson and Besson, 1992).

When the 002 peaks are considered, the situation is even better (Figure 1b). As their positions are separated by ~0.65°2θ, a nearly complete splitting of the two elementary peaks is observed even in the raw diffraction patterns and both graphical and fitting/decomposition-based FWMH measurements are possible and equally reliable.

In samples containing an intermediate K/Na mica, the problems are similar, though worsened by a lesser separation of the peaks (Figure 1a′). For the 10 Å reflections, such a separation is only 0.18–0.20°2θ; therefore the $KI_{10\,Å}$ values determined graphically on the un-decomposed complex peak appear significantly greater than those measured on decomposed peaks (samples 57 and 58); obviously, when the amounts of intermediate K/Na mica are low (as in samples 54 and 56), the effect of this phase on the illite peak is faint, as suggested by the good agreement between values graphically evaluated and values derived from the fitting/decomposition procedure. Measurements on the illite 002 reflection appear definitely more reliable, probably also when the interfering phase is very abundant, as the two reflections are separated by 0.35–0.40°2θ; in our samples 57 and 58 (Figure 1b′), where K/Na mica is abundant (though not dominant), the raw XRD pattern shows a fairly distinct hump-like reflection on the high-angle side of the illite peak, which still permits a good graphical evaluation of $KI_{5\,Å}$ value. Also, the decomposition procedure is made easier and more reliable here with respect to the 001 peak by an improved fitting quality.

Measurement of $KI_{10Å}$ and $KI_{5Å}$ in (illite + chlorite + illite-smectite) clay mineral assemblages

As will be discussed in detail in the paragraph on the nature of illitic materials, all the illite-smectite mixed-layer minerals present in our samples are highly illitic phases (I% >85) characterized by an ISII type of ordering. This is in good agreement with the metamorphic grade of the sample set having the illite + chlorite + illite-smectite assemblage, which ranges from late diagenesis to early-middle anchizone (Árkai, 2002). The presence of these swelling components produces in the XRD profiles from AD preparations a broadening of the illite 001 peak which manifests itself as a tail (Figures 2 and 3) or an evident bulge (Figure 4) on the low-angle side, which evolves into a broad band in the samples where these phases are more abundant and relatively richer in smectite (Figure 5). Ethylene glycol solvation results in a sharpening of the complex peak due to the shift towards lower angles of two contributions from the I-S phases. In the fitted and decomposed EG profiles, the first one, interpreted as a 001/001 reflection, appears as a low-intensity broad band (from ~5–9°2θ), which may only be appreciated in the I-S-richest samples (Figures 4 and 5), whereas in the poorer samples it is faint (Figure 3) or even hidden in the background (Figure 2); though variable, its maximum is frequently around 7.6°2θ (11.6 Å), which would indicate a component of the fourth-order peak of a 47 Å super-

https://doi.org/10.1346/CCMN.2004.0520109 Published online by Cambridge University Press

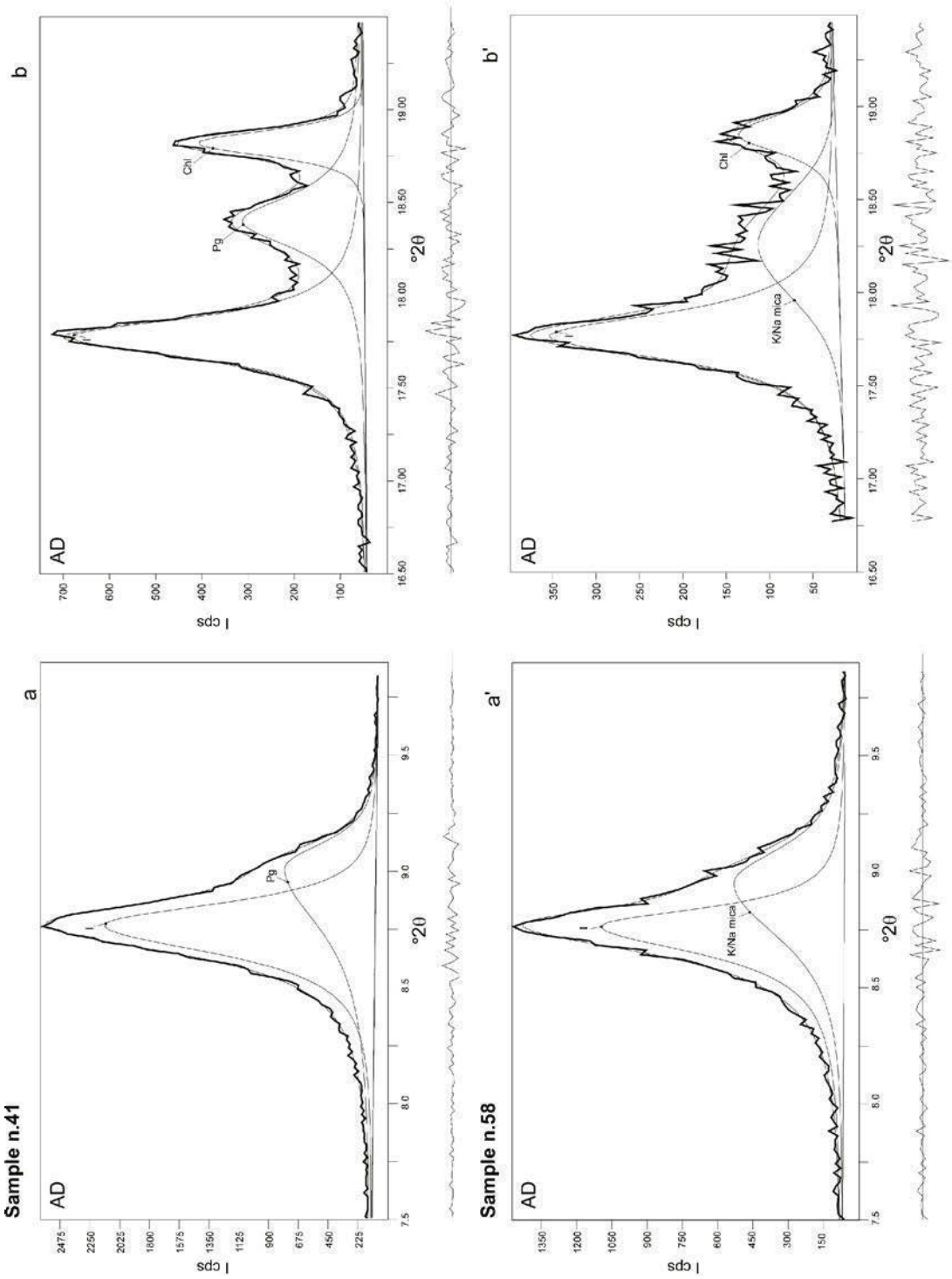

Figure 1. Decomposition of the XRD patterns obtained from air-dried (AD) preparations of samples containing the illite + chlorite + paragonite (sample n. 41) or the illite + chlorite + intermediate K/Na mica (sample n. 58) assemblages (a and a′: ~10 Å complex peak; b and b′: ~5 Å complex peak). In sample 41 it is likely that small amounts of an intermediate K/Na mica are also present; this would explain the asymmetry toward the low angles of the paragonite first reflection (Figure 1a).

https://doi.org/10.1346/CCMN.2004.0520109 Published online by Cambridge University Press

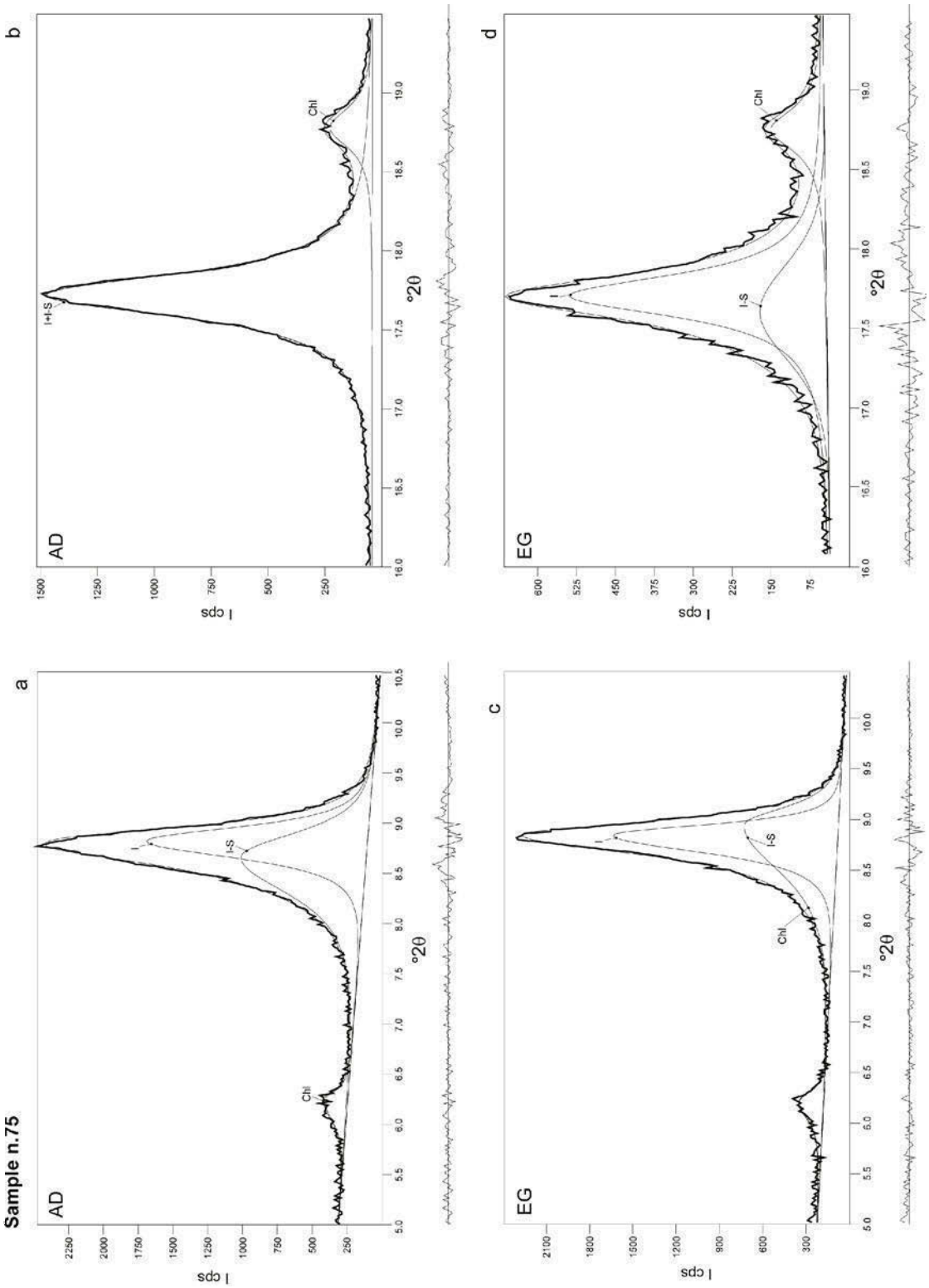

Figure 2. Decomposition of the XRD patterns obtained from air-dried (AD) and glycolated (EG) preparations of a sample (n. 75) containing moderately abundant amounts of smectite-poor illite-smectite mixed-layer minerals associated with illite and chlorite (a and c: ~10 Å complex peak; b and d: ~5 Å complex peak).

https://doi.org/10.1346/CCMN.2004.0520109 Published online by Cambridge University Press

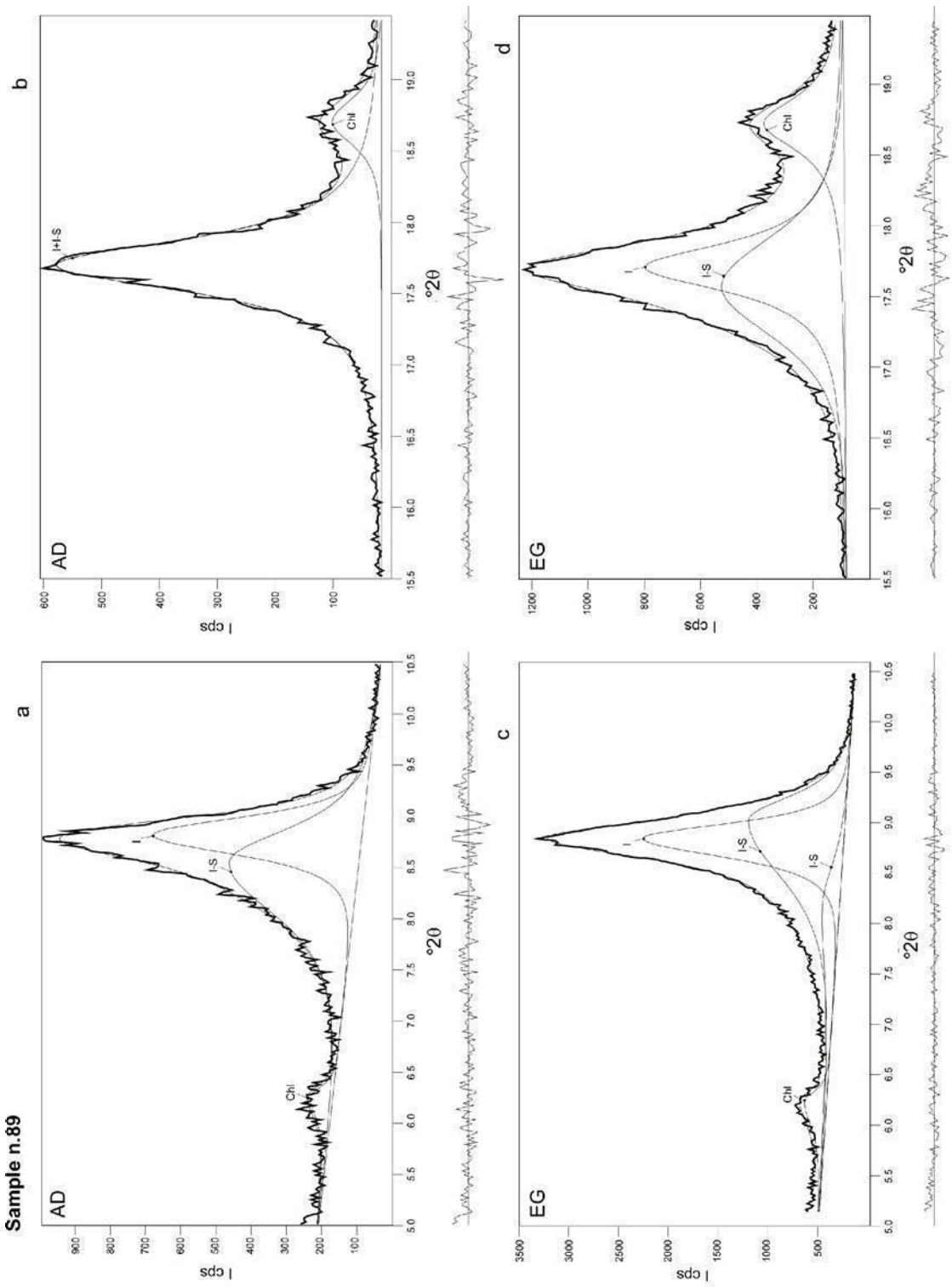

Figure 3. Decomposition of the XRD patterns obtained from air-dried (AD) and glycolated (EG) preparations of a sample (n. 89) containing abundant amounts of illite-smectite mixed-layer minerals associated with illite and chlorite; these mixed-layer minerals are slightly richer in smectite than those of sample n. 75 (a and c: ~10 Å complex peak; b and d: ~5 Å complex peak).

https://doi.org/10.1346/CCMN.2004.0520109 Published online by Cambridge University Press

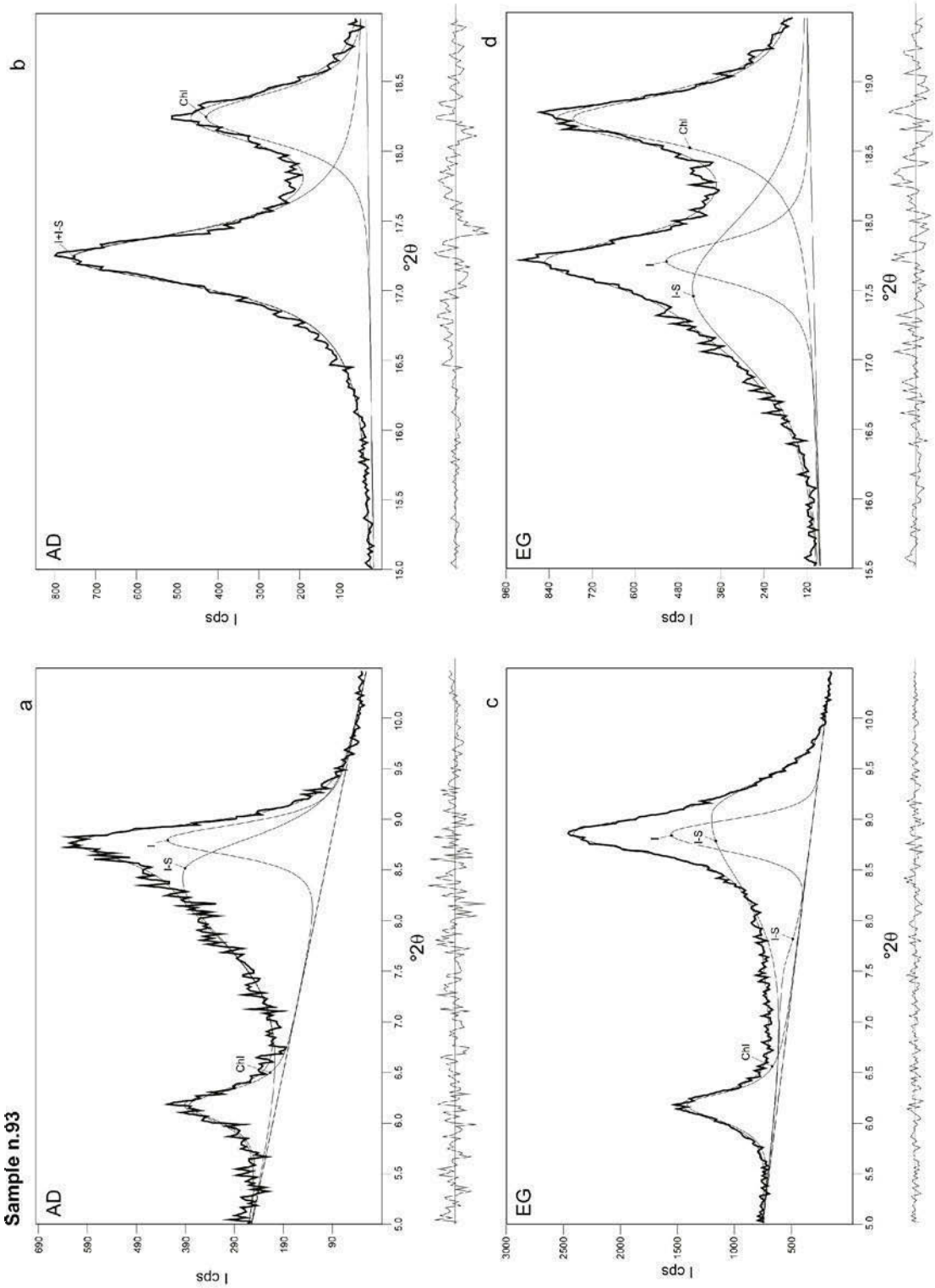

Figure 4. Decomposition of the XRD patterns obtained from air-dried (AD) and glycolated (EG) preparations of a sample (n. 93) containing abundant amounts of illite-smectite mixed-layer minerals associated with illite and chlorite; the mixed-layer minerals are relatively rich in smectite layers (a and c: ~10 Å complex peak; b and d: ~5 Å complex peak).

https://doi.org/10.1346/CCMN.2004.0520109 Published online by Cambridge University Press

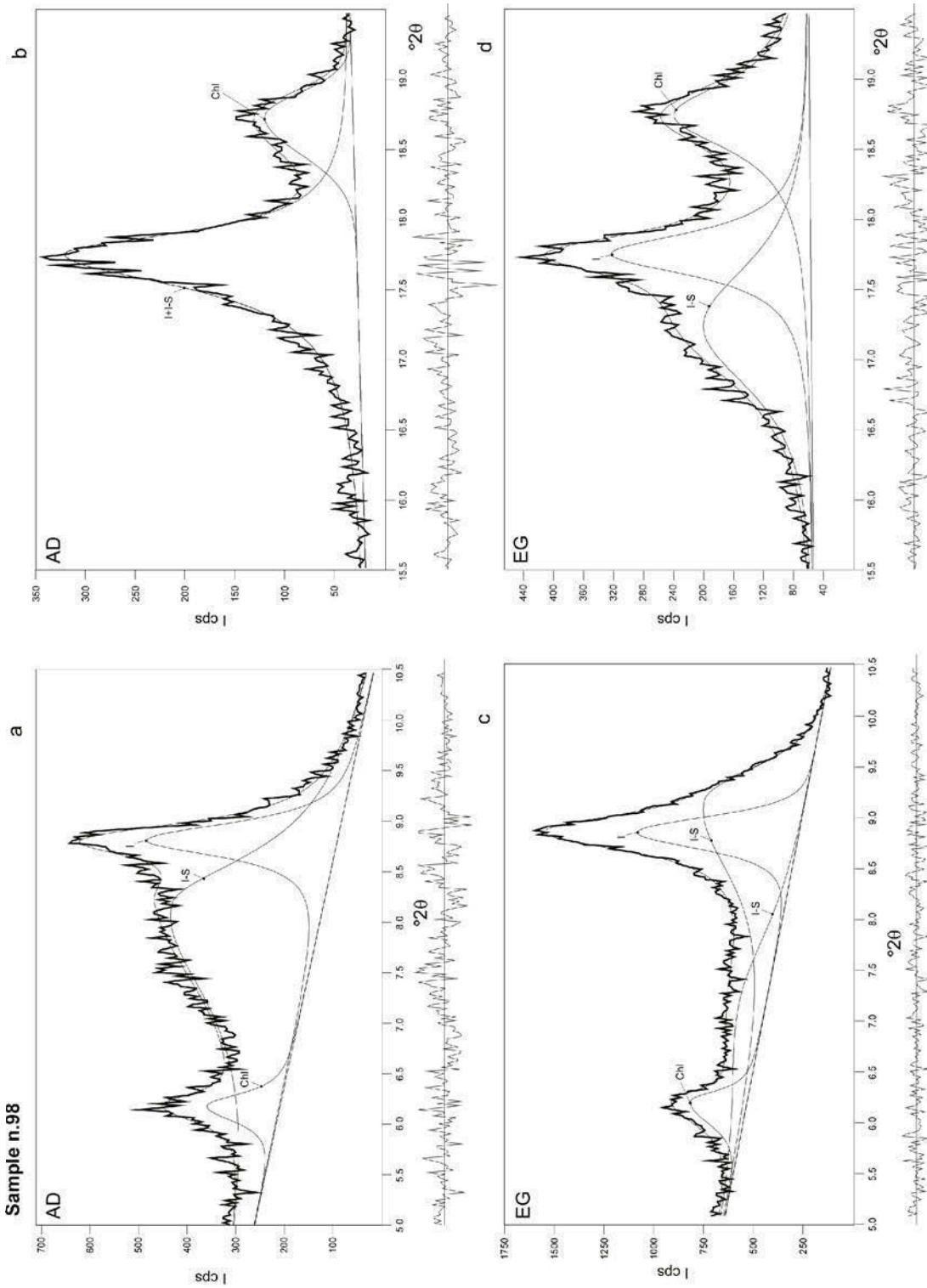

Figure 5. Decomposition of the XRD patterns obtained from air-dried (AD) and glycolated (EG) preparations of a sample (n. 98) containing very abundant amounts of illite-smectite mixed-layer minerals associated with illite and chlorite; these mixed-layer minerals are the richest in smectite of all the analyzed samples (see Table 2) (a and c: ~10 Å complex peak; b and d: ~5 Å complex peak).

https://doi.org/10.1346/CCMN.2004.0520109 Published online by Cambridge University Press

structure (Moore and Reynolds, 1997). The second contribution from the I-S phases is always appreciable in the EG-fitted and decomposed profiles, where it appears much more sharp and intense than the first one; its maximum ranges from 8.9 to 9.1°2θ (9.94 to 9.72 Å), which is consistent with a 001/002 reflection. This reflection is not appreciable in the complex 10 Å (AD) peak, where it is likely to have very low intensities. As a consequence, a good fitting of this peak could be obtained through a unique function, which describes the micaceous phase, in all the samples where the amounts of I-S minerals are low and/or these phases are smectite-poor (a condition indicated by a difference between $KI_{AD\text{-}10\ Å}$ and $KI_{EG\text{-}10\ Å}$ of <~0.04°2θ), through two functions (describing the illite 001 and the I-S 001/001 reflections, respectively) in the samples having from moderate to abundant amounts of expanding phases (*i.e.* where $KI_{AD\text{-}10\ Å} - KI_{EG\text{-}10\ Å}$ is >~0.04°2θ).

When the 5 Å peak is considered, the situation is definitely clearer. In all cases the AD peak can be fitted with a unique curve, due to a complete overlap of the illite 001 and I-S 002/003 reflections. On the contrary, the EG peak shows a more or less evident splitting of the two reflections. Whenever the expandability is low (a condition indicated by a difference between $KI_{AD\text{-}5\ Å}$ and $KI_{EG\text{-}5\ Å}$ of <0.08°2θ), the peak can still be fitted with a unique curve with an acceptable reliability (in most cases >95%). Whenever the expandability is from moderate to high, as shown by an evident asymmetry, or even a bulge, on the lower-angle side of the EG-5 Å peak and a difference of $KI_{AD\text{-}5\ Å} - KI_{EG\text{-}5\ Å}$ of >0.08°2θ, the application of two curves becomes compulsory. The two peaks are separated enough (from 0.10 to 0.50°2θ in position and more than 0.35°2θ in width) to allow for reliable measurements of FWHM on the illite decomposed reflection.

Measurement of $KI_{10Å}$ and $KI_{5Å}$ in (illite + chlorite + intermediate K/Na mica + illite-smectite) clay mineral assemblages

Dealing with samples which simultaneously contain an intermediate K/Na mica and a I-S mixed-layer mineral is a complicated matter. Two XRD profiles from samples having variable amounts of these phases are reported in Figures 6 and 7. The shape of the complex 10 Å peak from both AD and EG preparations are not manifestly different from that shown by samples having only I-S as a minor phase associated with the dominant illite and chlorite. However, the presence of an intermediate K/Na mica is indicated in the 5 Å region by the high saddle connecting illite 002 and chlorite 003 peaks, a diffraction effect which does not shift upon glycol solvation. Such a presence is established with an even greater reliability through examination of the angular range 26–28°2θ (not shown in Figures 6–7), where it produces a fairly distinct shoulder on the high-angle side of the illite 003 peak.

The complex peak around 10 Å (AD preparations), which appears large and markedly asymmetric towards the low angles, has been fitted with three curves. The first, which describes the I-S phase, shows an angular position variable with the amount of smectitic layers; in samples having a high expandability (sample 68, Figure 7) its effect is already quasi-resolved from the illite peak in the raw profile. The second curve and the third curve represent the illite and the K/Na mica, respectively. Actually, these two curves have characteristics (position and width) so close to be at the limits of the resolving power of the method; therefore, the fitting was run with constraints drawn from higher-order reflections or from other XRD patterns. The EG solvation causes the disappearance of the low-angle tail (since the I-S effect migrates towards lower angles to form the broad band from 6 to 8.5°2θ) and the appearance of a marked asymmetry at the high-angle side. This latter is due to the emergence of a composite peak resulting from the overlapping of K/Na mica 001 and I-S 001/002 reflections: this can only be fitted with a unique curve that has a position slightly shifted towards higher angles with respect to the peak of discrete K/Na mica observed in the AD patterns.

The possibility to separate elementary peaks of all the phases of this complex clay mineral assemblage is achieved only in the treatment of the 5 Å peak. In AD profiles, this peak is decomposed with two curves: the first one represents both illite and the I-S mixed-layer mineral, whose diffraction effects are perfectly overlapped (as also pointed out in the case of the assemblage described previously); the second curve represents the contribution of the intermediate K/Na mica. In EG profiles, discrimination of all the contributions is possible and the 5 Å peak is decomposed in three well-resolved curves (besides the curve fitting chlorite 003 reflection).

The relationship between $KI_{10Å}$ and $KI_{5Å}$

At first, investigation of the relationship between $KI_{10\ Å}$ and $KI_{5\ Å}$ was performed through data collected in the (illite ± chlorite) clay mineral assemblage. Samples characterized by this assemblage produce, in fact, XRD profiles where illite 001 and 002 peaks are virtually free of any interference from associated phases, thus affording KI measurements unaffected by such a major disturbing factor and not influenced at any grade by decomposition procedures. All the pairs (94) of KI values determined on both AD and EG mounts in the 47 samples with this assemblage have been applied to the regression analysis. This recorded an excellent linear correlation ($r^2 = 0.98$) expressed by the equation:

$$KI_{10\ Å} = KI_{5\ Å} \times 1.0921 - 0.0016°2\theta \quad (1)$$

Subsequently, investigation of the relationship was also tentatively extended to the other clay minerals assemblages by application of data acquired through

https://doi.org/10.1346/CCMN.2004.0520109 Published online by Cambridge University Press

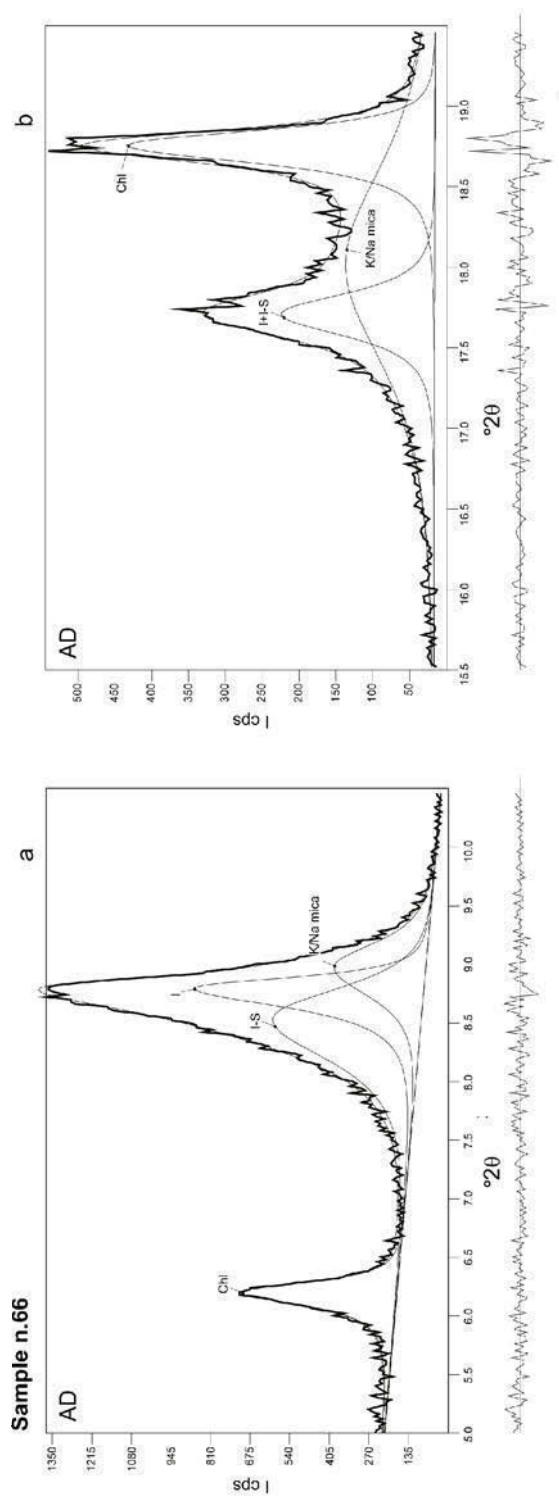

Figure 6. Decomposition of the XRD patterns obtained from air-dried (AD) and glycolated (EG) preparations of a sample (n. 66) containing the illite + chlorite + intermediate K/Na mica + illite-smectite assemblage; the I-S mixed-layer minerals are relatively poor in smectite layers (a and c: ~10 Å complex peak; b and d: ~5 Å complex peak).

https://doi.org/10.1346/CCMN.2004.0520109 Published online by Cambridge University Press

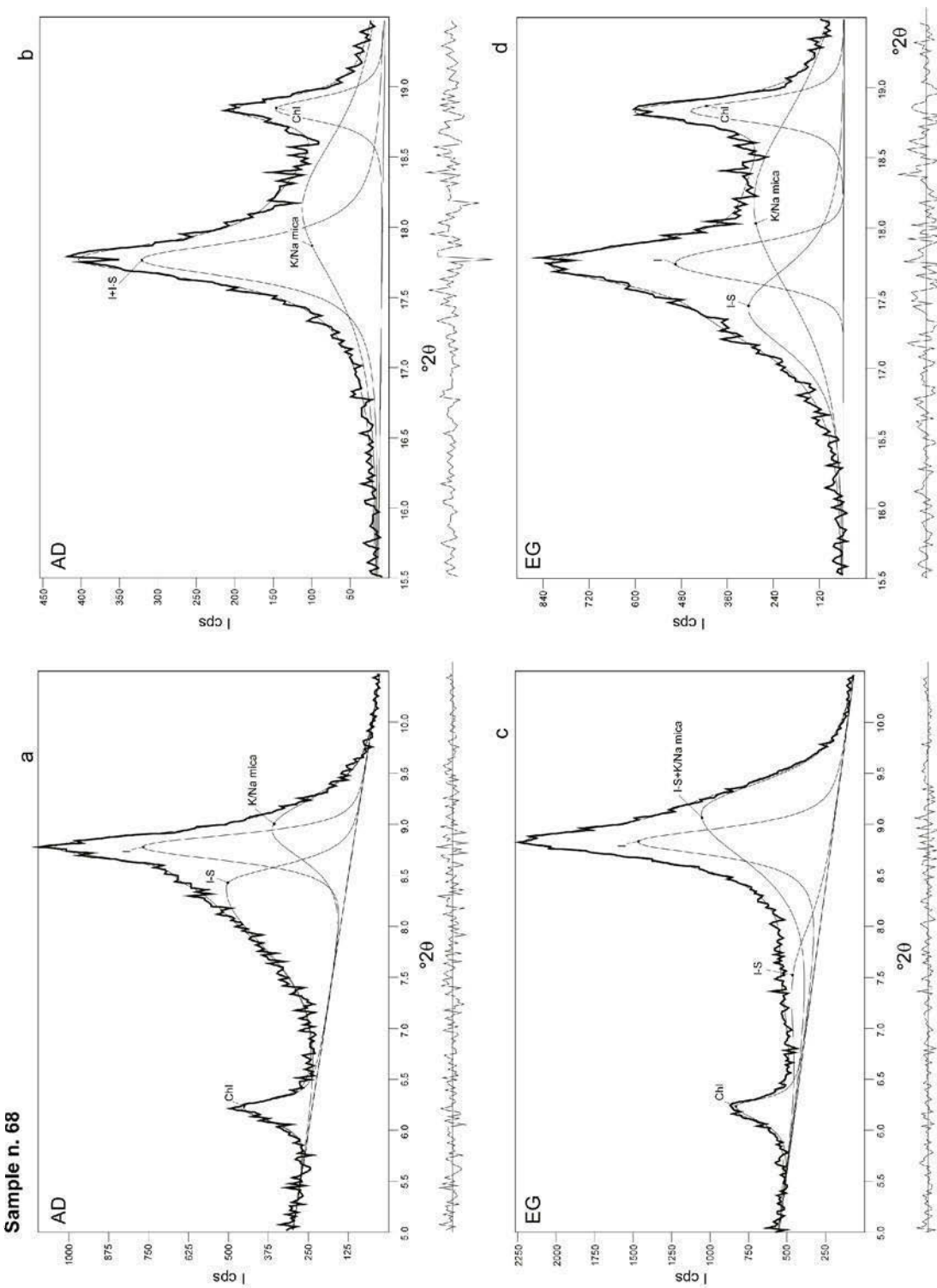

Figure 7. Decomposition of the XRD patterns obtained from air-dried (AD) and glycolated (EG) preparations of a sample (n. 68) containing the illite + chlorite + intermediate K/Na mica + illite-smectite assemblage; the I-S mixed-layer minerals are relatively rich in smectite layers (a and c: ~10 Å complex peak; b and d: ~5 Å complex peak).

https://doi.org/10.1346/CCMN.2004.0520109 Published online by Cambridge University Press

peak decomposition procedures. All the pairs of values thus obtained (except for $KI_{AD\text{-}10\ Å}$ and $KI_{AD\text{-}5\ Å}$ values from assemblages containing I-S minerals, whose illite 5 Å (AD) peak cannot be decomposed from the I-S 002/003 diffraction effect) were then added to the previous 94 to get a total of 166 couples of values. The regression analysis applied to this database yielded a good linear correlation (r^2 = 0.97) between the two parameters, which is expressed by the equation:

$$KI_{10\,Å} = KI_{5\,Å} \times 0.965 + 0.023°2\theta \quad (2)$$

From the first equation we can observe the tendency for the 5 Å peak to be slightly narrower than the 10 Å peak for every peak-width value. From the second equation we infer that the 5 Å peak is slightly narrower than the 10 Å peak for small-width values (in the range 0.10–0.50°2θ), whereas it becomes relatively broader for the larger widths, as diffraction theory predicts for higher 2θ angle peaks.

However, the difference between $KI_{10\,Å}$ and $KI_{5\,Å}$ is actually very small. If the smallest and largest $KI_{10\,Å}$ values recorded in our sample set (0.13 and 0.52°2θ, respectively) are considered, application of the regression equation 1 merely implies addition of 0.01 and 0.04°2θ to the first and the second values, respectively, whereas application of the equation 2 results in the addition of 0.02 and 0.005 to the first and the second values, respectively. These quantities are comparable with the errors associated with carefully performed measurements, as given by Warr and Rice (1994). This would mean that both peaks may be used interchangeably. However, we would prefer to perform the KI measurements on the 5 Å (EG) peak, since this reflection allows an easier and more complete decomposition of the contributions from all the possible interfering phases; the validity of this choice is probably better appreciated in cases where illite is associated with many abundant interfering phases.

The relation between $KI_{10\,Å}$ and $KI_{5\,Å}$ was previously investigated by Nieto and Sanchez Navas (1994) and by Warr (1996). The first authors analyzed this relation in a sample set (78) from various diagenetic and sub-greenschist sequences with the indication of other additional ~10 Å phases. Though strongly affected by the presence of several interfering phases (paragonite, I-S mixed-layer minerals, intermediate K/Na mica), their data gave best-fit regressions which are very close to a 1:1 linear curve, as expressed by the linear and the polynomial equations: $KI_{10\,Å} = KI_{5\,Å} \times 0.96 + 0.02°2\theta$; $KI_{10\,Å} = -[(KI_{5\,Å})^2 \times 0.62] + [(KI_{5\,Å}) \times 1.32] - 0.03°2\theta$ (Nieto and Sanchez Navas, 1994); these relationships, in particular the first one, are identical to equation 2 found in the present paper. Warr (1996), who utilized a smaller sample set (14) from similar metamorphic grades, still in part contaminated by I-S mixed-layer minerals or by discrete smectite, recorded a good linear correlation (r^2 = 0.974) expressed by the equation: $KI_{5\,Å} = KI_{10\,Å} \times 0.774 + 0.0354$; this linear fit shows a distinctly smaller slope than those recorded in the present paper and in the work by Nieto and Sanchez Navas (1994).

The nature of illitic materials

To characterize the illitic materials in a selected number of samples, the following parameters suggested by Środoń (1984) have been determined: the positions of the illitic material basal reflections in the range 4–40°2θ (EG mounts); $\Delta_{002-001}$ = the angular distance between the 002 and 001 reflections; BB1 = the joint breadth of 001 illite and adjacent I-S reflections; BB2 = the joint breadth of 004 illite and adjacent I-S reflections; Ir = the intensity ratios (peak heights ratios) of the 001 and 003 reflections from the AD and EG mounts, *i.e.* $[001_{AD}/003_{AD}]/[001_{EG}/003_{EG}]$; S% = the percentage of smectitic layers in I-S mixed-layer minerals. The BB1, BB2 and Ir parameters were determined graphically on chart-strip XRD patterns on un-decomposed complex peaks; all the other parameters were obtained from fitted and decomposed XRD profiles. These parameters are reported in Table 2.

In the first two clay mineral assemblages (of epizonal, middle-upper anchizonal, or, more rarely, upper diagenetic origin), the illitic material is made up of discrete illite, as indicated by a $\Delta_{002-001}$ value of 8.85–9.00°2θ and an Ir value of ~1 (Środoń, 1984). This latter parameter is very sensitive to the appearance of an expanding component, which would be indicated by values >1. So, the diagenetic samples 76 and 80, which have an Ir value of 1.10 though not showing any discrete I-S basal reflection even in fitted and decomposed XRD profiles, are likely to contain trace amounts of I-S minerals associated with a dominant illite population.

In the two remaining clay mineral assemblages (of lower anchizonal to upper diagenetic origin), the I-S minerals are present in small to large amounts, as indicated by Ir values significantly greater than 1 and $\Delta_{002-001}$ values (for the discrete I-S phase) <8.7°2θ (Środoń, 1984). These minerals are highly illitic phases, as indicated by their low content of smectite layers, which range from 6 to 12% (according to Środoń, 1984, the value reported in column B of Table 2 is more reliable than that listed in column A). Furthermore, they appear as highly ordered mixed-layer phases of the ISII type, as suggested by BB1 and BB2 values <4°2θ (Środoń, 1984).

The use of KI data from decomposed complex peaks in the assessment of metamorphic grade

As pointed out in the introduction, among the aims of the present work was the search for a KI measurement procedure which could give values not affected by the presence of interfering phases. In the previous paragraphs it has been shown that the measurements performed on the decomposed 5 Å peak in XRD patterns from glycolated mounts represent the best choice for this

https://doi.org/10.1346/CCMN.2004.0520109 Published online by Cambridge University Press

purpose. The $KI_{5\,Å}$ values so acquired can be converted into $KI_{10\,Å}$ values through application of or equations 1 or 2 (the latter is preferable); though only producing variations which are within error limits, this conversion is recommended in order to avoid systematic (though small) errors in the measurement procedure.

The $KI_{10\,Å}$ values thus obtained must be regarded as FWHM values from a micaceous population with a mean crystallite thickness, since in our decomposition procedure we did not apply the two curves suggested by Lanson (1997) and Lanson and Besson (1992) to illite to account for a sub-population of crystallites of low thickness and a sub-population of crystallites of high thickness.

The subsequent step, *i.e.* correlating these values with Kübler's original KI scale is not straightforward; it requires caution and an accurate re-calibration of Kübler's scale limits. This was stressed by Árkai (2002), who observed that an application of KI values from decomposition procedures to Kübler's scale may lead to conflicting results. Here, just a few general observations on the question will be drawn from data presented in Tables 1 and 3. In Table 1 it is clearly seen that graphically-derived parameters (in particular $KI_{AD\text{-}10\,Å}$) are affected by a wide scatter of values in comparison with all the parameters obtained through fitting/decomposition procedures. This pattern is progressively more evident with decreasing metamorphic grade, from the middle–low anchizone to the diagenetic zone. On the contrary, all the parameters obtained through fitting/decomposition procedures have values much more similar to each other (in particular those measured on 5 Å (EG) peak), which appear consistent with measurements performed on samples belonging to the same population, but lacking mixed-layer minerals.

In Table 3 the average KI values for the studied sample sets, calculated from the data in Table 1, are reported. In the last two columns, the computer-derived values measured on the decomposed 5 Å (EG) reflection, converted to the 10 Å peak through the equation $KI_{10\,Å} = KI_{5\,Å} \times 0.965 + 0.023°2\theta$ and calibrated with respect to Kübler's standards through the equation $KI_{Kübler} = KI_{Pisa} \times 1.08 + 0.01°2\theta$ (column A), are compared with the graphically-derived values determined on the un-decomposed 10 Å (AD) peak, also calibrated with respect to Kübler's standards (column B). This table clearly shows that in epizonal and upper anchizonal sample populations there is no significant difference between the A and B values. From the middle anchizone to the diagenetic zone (graphically-measured $KI_{AD\text{-}10\,Å}$ values >0.30) the two values become increasingly different, with the exception of population 8, which records identical values due to a clay mineral assemblage essentially made up of illite and chlorite. The maximum divergence is shown by population 10, which exhibits average values of 0.43 and 0.90°2θ for the parameters of the A and B columns, respectively. The first value would ascribe the sample population to the anchizone/diagenesis transition, whereas the second one would suggest middle–early diagenetic conditions. Preliminary data reported in the literature for this sample population (see Appendix at Internet site: http://www.dst.unipi.it/min/clay), in particular the type of calcite twinning, seem to indicate the first assessment as being more correct.

Also population 9, which includes all the samples collected in the Bracco/Val Graveglia Unit, shows contrasting values of KI in A and B columns (0.49 and 0.66°2θ, respectively). The first value would point to late diagenetic conditions, not far from the diagenesis/anchizone transition; the second one would indicate a distinctly lower metamorphic grade. The prehnite-pumpellyite facies of the metabasites associated with the Palombini Shale in this unit and the results of a study by Leoni *et al.* (1996) (see Appendix at Internet site: http://www.dst.unipi.it/min/clay) would confirm late diagenesis as the most probable grade.

The case of population 6 is particularly interesting, since it groups together all the samples collected in the Tuscan Nappe Unit from three different formations. As already pointed out, all these formations are supposed to have the same metamorphic grade since the difference between their structural depths is rather small (250–400 m; Carosi *et al.*, 2003). However, the $KI_{10\,Å}$ parameter of column B records widely scattering values, which range from 0.29 to 0.57°2θ; this would point to grades ranging from upper anchizone (not far from the epizone/anchizone transition) to diagenesis. On the contrary, the $KI_{10\,Å}$ parameter from fitted and decomposed profiles (column A) shows values relatively close to each other (0.27–0.32°2θ). This pattern is a consequence of the distribution of interfering phases (see Table 1). The clay mineral assemblage of the Posidonomya Marl Formation contains only illite and chlorite, whereas the other two formations contain more or less abundant I-S mixed-layer minerals and K/Na intermediate micas. The presence of these phases greatly affects the measurements performed graphically on the un-decomposed 10 Å (AD) peaks (values of column B), whereas it should not influence the FWHM evaluations on illite fitted and decomposed peaks (values of column A).

As to the differences in clay mineral assemblages between formations supposed to have the same metamorphic grade, it is reasonable to ascribe them to differences in lithology. The Rhaetavicula contorta Limestone and Marl Formation has lithologies characterized by significant contents of organic matter (see Appendix at Internet site: http://www.dst.unipi.it/min/clay), which may be the cause of an appreciable delay in phyllosilicate aggradation (Frey, 1987). The Tuscan Scaglia Formation is characterized by considerable amounts of Na in the bulk composition of the clay fraction; this is expressed by the abundance of K/Na

https://doi.org/10.1346/CCMN.2004.0520109 Published online by Cambridge University Press

intermediate micas and probably implies a sodic character of the smectitic component in the I-S mixed-layer minerals. According to Mullis *et al.* (2002), this situation, deriving from early diagenetic high-saline fluids, would result in a delay in the smectite to illite reaction progress. Therefore we believe the data collected on the Posidonomya Marl Formation to be the most reliable for the assessment of the whole Tuscan Nappe Unit metamorphic grade, as it is confirmed by the temperature values derived through carbonate thermometry (Carosi *et al.*, 2003), fluid inclusion analysis (Montomoli *et al.*, 2001) and vitrinite reflectance data (Reutter *et al.*, 1980). These data from the Posidonomya Marl Formation appear to be in acceptable agreement with those collected through the fitting/decomposition procedure in the other two formations. We can then conclude that also in the case of population 6 the KI measurements performed through the fitting/decomposition procedure seem to produce a better estimation of the metamorphic grade than traditional measurements.

CONCLUSIONS

By comparing traditional measurements of illite Kübler index (graphical evaluations on un-decomposed peaks from chart-strip XRD patterns) with those obtained from fitted and decomposed peaks the following conclusions can be drawn:

(1) At relatively high metamorphic grades (from the upper anchizone to the epizone), the clay mineral assemblages are commonly very simple, most of them containing only illite and chlorite, sometimes associated with minor amounts of paragonite. On these assemblages, the KI measurements through the two procedures are equally reliable. However, when the amounts of paragonite are important, the fitting/decomposition procedure becomes compulsory.

(2) At very low metamorphic grades (from diagenesis to the middle anchizone), the clay mineral assemblages are more complex and require application of the fitting/decomposition procedure to de-sum the contributions of several interfering phases from the illitic material diffraction effects.

(3) KI measurements on the 5 Å peak in XRD profiles from glycolated mounts seem the best choice in comparison with those performed on the 10 Å peak, since the former is the reflection which allows an easier and more complete decomposition of the contributions from all the possible interfering phases.

(4) The relationship between $KI_{10\,Å}$ and $KI_{5\,Å}$ appears very close to a 1:1 linear relation, the difference between the two parameters being within error limits. Nevertheless, the conversion from $KI_{5\,Å}$ to $KI_{10\,Å}$ through the appropriate equation is recommended in order to avoid a small, but systematic error.

(5) The KI values obtained from complex peak decomposition through the proposed procedure are consistent with those obtained from samples of the same population and the same metamorphic grade, which lack interfering phases.

(6) In the range late diagenesis–middle anchizone, where I-S mixed-layer minerals, K/Na intermediate micas and other interfering phases are common, KI values acquired through the proposed procedure seem to allow better estimates of the metamorphic grade than those obtained from traditional KI measurements.

REFERENCES

Árkai, P. (2002) Phyllosilicates in very low-grade metamorphism: Transformation to micas. Pp. 463–478 in: *Micas: Crystal Chemistry and Metamorphic Petrology* (A. Mottana, F.P. Sassi, J.B. Thompson and S. Guggenheim, editors). Reviews in Mineralogy and Geochemistry, **46**. Mineralogical Society of America, Washington, D.C.

Árkai, P., Sassi, F.P. and Sassi, R. (1995) Simultaneous measurements of chlorite and illite crystallinity: a more reliable tool for monitoring low- to very low-grade metamorphism in metapelites. A case study from the Southern Alps (NE Italy). *European Journal of Mineralogy*, **7**, 1115–1128.

Carosi, R., Leoni, L., Montomoli, C. and Sartori, F. (2003) Very low-grade metamorphism in the Tuscan Nappe, Northern Apennines, Italy: relationships between deformation and metamorphic indicators in the La Spezia mega-fold. *Schweizerische Mineralogische und Petrographische Mitteilungen*, **83**, (in press).

Frey, M. (1987) Very low-grade metamorphism of clastic sedimentary rocks. Pp. 9–58 in: *Low temperature Metamorphism* (M. Frey, editor). Blackie, Glasgow & London.

Frey, M. and Robinson, D. (1999) *Low-grade Metamorphism*. Blackwell Science, Oxford, UK, 313 pp.

Guggenheim, S., Bain, D.C., Bergaya, F., Brigatti, M.F., Drits, V.A., Eberl, D.D., Formoso, M.L.L., Galán, E., Merriman, R.J., Peacor, D.R., Stanjek, H. and Watanabe, T. (2002) Report of the Association International pour l'Étude des Argiles (AIPEA) nomenclature Committee for 2001: order, disorder and crystallinity in phyllosilicates and the use of the 'crystallinity index'. *Clays and Clay Minerals*, **50**, 406–409.

Kisch, H.J. (1990) Calibration of the anchizone: A critical comparison of illite "crystallinity" scales used for definition. *Journal of Metamorphic Geology*, **8**, 31–46.

Kisch, H.J. (1991) Illite crystallinity: recommendations on sample preparation, X-ray diffraction settings, and interlaboratory samples. *Journal of Metamorphic Geology*, **9**, 665–670

Kisch, H.J. and Frey, M. (1987) Appendix: Effect of sample preparation on the measured 10 Å peak width of illite (illite "crystallinity"). Pp. 301–304 in: *Low-temperature Metamorphism* (M. Frey, editor). Blackie, Glasgow & London.

Kretz, R. (1983) Symbols for rock-forming minerals. *American Mineralogist*, **68**, 277–279.

Krumm, S. (1992) Illitkristallinität als Indikator schwacher Metamorphose. Metodische Untersuchungen, regionale Anwendungen und Vergleiche mit anderen Parametern. *Erlanger Geologische Abhandlungen*, **120**, 1–75.

Krumm, S. (1996) WINFIT 1.2: version of November 1996 (The Erlangen geological and mineralogical software collection) of "WINFIT 1.0: a public domain program for interactive profile-analysis under WINDOWS". XIII Conference on Clay Mineralogy and Petrology, Praha,

https://doi.org/10.1346/CCMN.2004.0520109 Published online by Cambridge University Press

1994. *Acta Universitatis Carolinae Geologica*, **38**, 253–261.

Krumm, S. and Buggisch, W. (1991) Sample preparation effects on illite crystallinity measurement: Grain-size gradation and particle orientation. *Journal of Metamorphic Geology*, **9**, 671–677.

Krumm, S., Kisch, H.J. and Warr, L.N. (1994) Inter-laboratory study of the effects of sample preparation on illite "crystallinity": A progress report. XIII Conference on Clay Mineralogy and Petrology, Praha 1994. *Acta Universitatis Carolinae Geologica*, **38**, 263–270.

Kübler, B. (1964) Les argiles, indicateurs de métamorphisme. *Revue de l'Institut Français du Pétrole*, **19**, 1093–1112.

Kübler, B. (1967) La cristallinité de l'illite et les zones tout à fait supérieures du métamorphisme. Pp. 105–121 in: *Etages tectoniques, Colloque de Neuchâtel 1966*, Editions de la Baconnière, Neuchâtel, Switzerland.

Kübler, B. (1984) Les indicateurs des transformations physiques et chimiques dans la diagenèse, température et calorimétrie. Pp. 489–596 in: *Thermobarométrie et Barométrie Géologiques* (M. Lagache, editor). Société Française de Minéralogie et Cristallographie, Paris.

Lanson, B. (1990) Mise en évidence des mécanismes de transformation des interstratifiés illite/smectite au cours de la diagenèse. PhD thesis, Université de Paris 6-Jussieu, Paris, France, 366 pp.

Lanson, B. (1997) Decomposition of experimental X-ray diffraction patterns (profile fitting): a convenient way to study clay minerals. *Clays and Clay Minerals*, **45**, 132–146.

Lanson, B. and Besson, G. (1992) Characterization of the end of smectite-to-illite transformation: Decomposition of X-ray patterns. *Clays and Clay Minerals*, **40**, 40–52.

Lanson, B. and Champion, D. (1991) The I/S-to-illite reaction in the late stage diagenesis. *American Journal of Science*, **291**, 473–596.

Leoni, L. (2001) New standardized illite crystallinity data from low- to very low-grade metamorphic rocks (Northern Apennines, Italy). *European Journal of Mineralogy*, **13**, 1109–1118.

Leoni, L, Marroni, M., Sartori, F. and Tamponi, M. (1996) Metamorphic grade in metapelites of the Internal Liguride Units (Northern Apennines, Italy). *European Journal of Mineralogy*, **8**, 35–50.

Lezzerini, M., Sartori, F. and Tamponi, M. (1995) Effect of amount of material used on sedimentation slides in the control of illite 'crystallinity' measurements. *European Journal of Mineralogy*, **7**, 819–823.

Montomoli, C., Ruggieri, G., Boiron, M.C. and Cathelineau, M. (2001) Pressure fluctuations during uplift of the Northern Apennines (Italy): a fluid inclusion study. *Tectonophysics*, **341**, 121–139.

Moore, D.M. and Reynolds, R.C. (1997) *X-ray Diffraction and the Identification and Analysis of Clay Minerals*. Oxford University Press, Oxford-New York, 378 pp.

Mullis, J., Rahn, M.K., Schwer, P., de Capitani, C., Stern, W.B. and Frey, M. (2002) Correlation of fluid inclusion temperatures with illite "crystallinity" data and clay mineral chemistry in sedimentary rocks from the external part of the Central Alps. *Schweizerische Mineralogische und Petrographische Mitteilungen*, **82**, 325–340.

Nieto, F. and Sánchez-Navas, A. (1994) A comparative XRD and TEM study of the physical meaning of the white mica 'crystallinity' index. *European Journal of Mineralogy*, **6**, 611–621.

Reutter, K.J., Teichmüller, M., Teichmüller, R. and Zanzucchi, G. (1980) Le ricerche sulla carbonificazione dei frustoli vegetali nelle rocce clastiche, come contributo ai problemi di paleogeotermia e tettonica nell'Appennino Settentrionale. *Memorie della Società Geologica Italiana*, **21**, 111–126.

Robinson, D., Warr, L.N. and Bevins, R.E. (1990) The illite "crystallinity" technique: A critical appraisal of its precision. *Journal of Metamorphic Geology*, **8**, 333–344.

Środoń, J. (1984) X-ray powder diffraction identification of illitic materials. *Clays and Clay Minerals*, **32**, 337–349.

Stern, W.B., Mullis, J., Rahn, M. and Frey, M. (1991) Deconvolution of the first "illite" basal reflection. *Schweizerische Mineralogische und Petrographische Mitteilungen*, **71**, 453–462.

Velde, B. and Lanson, B. (1993) Comparison of I/S transformations and maturity of organic matter at elevated temperatures. *Clays and Clay Minerals*, **41**, 178–183.

Wang, H., Stern, W.B. and Frey, M. (1995) Deconvolution of the X-ray "Illite" 10-Å complex: A case study of Helvetic sediments from eastern Switzerland. *Schweizerische Mineralogische und Petrographische Mitteilungen*, **75**, 187–199.

Warr, L.N. (1996) Standardized clay mineral crystallinity data from the very low-grade metamorphic facies rocks of southern New Zealand. *European Journal of Mineralogy*, **8**, 115–127.

Warr, L.N. and Rice, A.H.N. (1994) Interlaboratory standardization and calibration of clay mineral crystallinity and crystallite size data. *Journal of Metamorphic Geology*, **12**, 141–152.

Weaver, C.E. (1960) Possible uses of clay minerals in search for oil. *Bulletin of the American Association of Petroleum Geologists*, **44**, 1505–1518.

(*Received 28 May 2003; revised 29 September 2003; Ms. 796*)

https://doi.org/10.1346/CCMN.2004.0520109 Published online by Cambridge University Press